EBioMedicine 25 (2017) 154–164

Contents lists available at ScienceDirect

EBioMedicine

journal homepage: www.ebiomedicine.com

Research Paper

Attenuation of $CD4^+CD25^+$ Regulatory T Cells in the Tumor Microenvironment by Metformin, a Type 2 Diabetes Drug

Yuki Kunisada [a,b], Shingo Eikawa [a], Nahoko Tomonobu [a], Shohei Domae [b], Takenori Uehara [a,c], Shohei Hori [d], Yukihiro Furusawa [e], Koji Hase [e], Akira Sasaki [b], Heiichiro Udono [a,*]

[a] Department of Immunology, Okayama University Graduate School of Medicine, Dentistry and Pharmaceutical Sciences, Okayama 700-8558, Japan
[b] Department of Oral and Maxillofacial Surgery, Okayama University Graduate School of Medicine, Dentistry and Pharmaceutical Sciences, Okayama 700-8558, Japan
[c] Department of Orthopaedic Surgery, Okayama University Graduate School of Medicine, Dentistry and Pharmaceutical Sciences, Okayama 700-8558, Japan
[d] Laboratory of Immunology and Microbiology, Graduate School of Pharmaceutical Sciences, The University of Tokyo, Tokyo 113-0033, Japan
[e] Division of Biochemistry, Keio University Graduate School of Pharmaceutical Science, Tokyo, Japan

ARTICLE INFO

Article history:
Received 19 April 2017
Received in revised form 4 October 2017
Accepted 9 October 2017
Available online 16 October 2017

Keywords:
Tumor immunity
Tumor microenvironment
Regulatory T cell (Treg)
Glycolysis
mTOR

ABSTRACT

$CD4^+CD25^+$ regulatory T cells (Treg), an essential subset for preventing autoimmune diseases, is implicated as a negative regulator in anti-tumor immunity. We found that metformin (Met) reduced tumor-infiltrating Treg (Ti-Treg), particularly the terminally-differentiated $CD103^+KLRG1^+$ population, and also decreased effector molecules such as CTLA4 and IL-10. Met inhibits the differentiation of naïve $CD4^+$ T cells into inducible Treg (iTreg) by reducing forkhead box P3 (Foxp3) protein, caused by mTORC1 activation that was determined by the elevation of phosphorylated S6 (pS6), a downstream molecule of mTORC1. Rapamycin and compound C, an inhibitor of AMP-activated protein kinase (AMPK) restored the iTreg generation, further indicating the involvement of mTORC1 and AMPK. The metabolic profile of iTreg, increased Glut1-expression, and reduced mitochondrial membrane-potential and ROS production of Ti-Treg aided in identifying enhanced glycolysis upon Met-treatment. The negative impact of Met on Ti-Treg may help generation of the sustained antitumor immunity.

1. Introduction

Metformin (Met), the most widely prescribed first-line drug for type 2 diabetes (T2D), is a low cost and relatively safe therapeutic that has recently garnered more attention because of its anticancer effects. Several epidemiologic studies have suggested that Met use may reduce cancer incidence in T2D patients and, moreover, improve their prognosis compared with those taking other drugs (Evans et al., 2005; Morales and Morris, 2015; Noto et al., 2012). Regarding the mechanism, Met has been suggested to directly inhibit the proliferation and invasion of tumor cells and/or cancer stem cells (Song et al., 2012; Hirsch et al., 2009; Shank et al., 2012), which could be explained by the downregulation of the mammalian target of rapamycin (mTOR) kinase signaling, following the activation of AMP-activated protein kinase (AMPK) in tumor cells (Han et al., 2015; Zheng et al., 2013; Nair et al., 2014). However, the plasma concentration of Met in T2D patients is significantly lower (<20 μM) than the doses used in most experimental settings, which could not explain the reduction of cancer incidence and/or mortality.

Aside from the direct effect of Met on cancer cells, the indirect mechanism including lowering glucose, insulin, and insulin-like growth factor in peripheral blood may be an alternative explanation, since those factors promote tumor cell proliferation and expansion (Renehan et al., 2006; Halje et al., 2012). Such indirect effects also involve our previous observations that oral administration of Met in drinking water caused the rejection of solid tumors or reduced their growth in mice. The Met-induced antitumor effect was mediated by the immune system because the effect was completely abrogated in T cell-deficient mice or by *in vivo* depletion of $CD8^+$ T cells by injection of a specific antibody (Eikawa et al., 2015). We found this occurred through the activation

Abbreviations: mTOR, mammalian target of rapamycin; Treg, T regulatory cell; FAO, fatty acid oxidation; Met, metformin; Ti-Treg, tumor infiltrating-T regulatory cell; CTLA4, cytotoxic T-lymphocyte-4; IL-10, interleukin-10; KLRG1, killer cell lectin-like receptor G1; CD103, Cluster Designation 103, Integrin αE; AMPK, AMP-activated protein kinase; iTreg, inducible T regulatory cell; Glut1, glucose transporter 1; T2D, type 2 diabetes; Foxp3, forkhead box P3; TGF-β, Transforming growth factor-β1; RA, rapamycin; CC, compound C; GFP, green fluorescent protein; OVA, Ovalbumin; TIL, tumor infiltrating lymphocyte; FITC, fluorescein isothiocyanate; APC, allophycocyanin; PE, phycoerythrin; FSC, forward scatter; SSC, side scatter; CFSE, carboxyfluorescein diacetate succinimidyl ester; CTV, cell trace violet; TMRE, tetramethylrhodamine ethyl ester; OCR, oxygen consumption rate; ECAR, extracellular acidification rate; FCCP, Carbonyl cyanide 4-(trifluoromethoxy) phenylhydrazone, potent mitochondrial oxidative phosphorylation uncoupler; TCR, T cell antigen receptor; ROS, Reactive oxygen species.

* Corresponding author at: Department of Immunology, Okayama University Graduate School of Medicine, Dentistry and Pharmaceutical Sciences, 2-5-1 Shikata-cho, Kita-ku, Okayama 700-8558, Japan.
E-mail address: udono@cc.okayama-u.ac.jp (H. Udono).

https://doi.org/10.1016/j.ebiom.2017.10.009

of tumor-infiltrating, exhausted $CD8^+$ T cells ($CD8^+$ TILs) that had lost most of the original functions, such as the ability to produce multiple cytokines and cytotoxicity. $CD8^+$ TILs of mice exposed to Met begin to rapidly produce multiple cytokines, including interleukin-2 (IL-2), tumor necrosis factor alpha (TNFα), and interferon gamma (IFNγ), and differentiate into effector memory T cells (TEM); otherwise, central memory T cells (TCM) are dominant in the tumor microenvironment. Since the plasma concentration of Met in mice is comparable with that in T2D patients (Memmott et al., 2010), the perspective on the immune system involvement might partly reconcile the significant anticancer effects with such a low plasma concentration of Met.

$CD4^+CD25^+$ regulatory T cells (Treg) has been implicated as a negative regulator for T cell mediated antitumor immunity (Nishikawa and Sakaguchi, 2010; Adeegbe and Nishikawa, 2013; Facciabene et al., 2012). In fact, depletion of Treg cells was shown to reject solid tumors or to reduce tumor growth (Onizuka et al., 1999; Shimizu et al., 1999). Therefore, the targeting of Treg cells is an attractive intervention for cancer immunotherapy (Kurose et al., 2015). In this study, we show that Met administration decreased the number of Treg cells, particularly terminally differentiated $KLRG1^+CD103^+$ Treg cells (Joshi et al., 2015) (*i.e.*, active effector Treg cells), at tumor sites but not in peripheral lymphoid tissues by inducing apoptosis. The effect paralleled with reprogramming of the metabolic state toward glycolysis and activation of mTORC1. Approximation of *in vitro* study showed that Met pretreatment of naïve $CD4^+CD25^-$ T cells blocked its differentiation into TGFβ dependent inducible Treg (iTreg) cells through downregulation of Foxp3, a master transcription factor for Treg cells (Hori et al., 2003; Fontenot et al., 2003). The Foxp3 downregulation *in vitro* also correlates with elevation of glycolysis over oxidative phosphorylation, as indicated by the results of Seahorse analyzer, and is dependent on activities of mTORC1 and AMPK since specific inhibitors, rapamycin (RA) and compound C (CC), restored the Foxp3 level, respectively. Thus, Met inhibits TGF-β-dependent differentiation of Treg cells, which in turn may generate a favorable state of sustained antitumor immunity in a tumor microenvironment.

2. Materials and Methods

2.1. Animals

BALB/c and C57BL/6 (B6) mice were purchased from SLC and CLEA Japan. $Foxp3^{GFP\text{-}cre}$ mice were used previously (Miyao et al., 2012). All mice were maintained in specific pathogen-free conditions in the animal facility of Okayama University. The studies have been approved by an Institutional Animal Care and Use Committee of Okayama University Graduate School of Medicine.

2.2. Tumor Cell Lines

BALB/c fibrosarcoma MethA, BALB/c radiation leukemia RLmale1, B6 fibrosarcoma MCA, and B6 OVA gene-transduced B16 melanoma MO5 were used for the tumor assay. These tumor cell lines were used previously (Eikawa et al., 2015), except MCA (Boissonnas et al., 2010).

2.3. Tumor Growth Assay

Mice were intradermally inoculated with tumor cells (MethA: 1.5×10^5, RLmale1: 2.0×10^5, MCA: 1.0×10^5, MO5: 2.0×10^5) on the right back with a 27-gauge needle. Mice were orally administered with Met hydrochloride (Tokyo Chemical Industry Co., Ltd., Japan) dissolved in drinking water (5 mg/mL). The long (a) and short (b) diameters of the tumors were measured with a Vernier caliper, and the tumor volume (V) was calculated according to the following equation: $V = a \times b^2/2$.

2.4. Isolation of TILs

Tumor tissues were dissected from the mice and minced into small pieces in RPMI 1640 medium (Life Technologies, Tokyo, Japan). TILs were harvested from the minced tumor tissues using a Medimachine system (AS ONE, Osaka, Japan). Lymphocytes (TILs) could be distinguished from tumor cells since their size is less than half of that of tumor cells under a microscope. Then, we stained all cells, including TILs and tumor cells, with the indicated fluorescence-labeled antibodies and subjected them to flow cytometric analysis.

2.5. $CD4^+CD25^-$ T Cell Separation, In Vitro Induction, and Expansion of iTreg Subsets

$CD4^+$ $CD25^-$ T cells were isolated from B6 spleen cells by magnetic separation (Miltenyi Biotec, Tokyo, Japan). $CD4^+CD25^-$ T cells were incubated with 10 μM Met or rotenone (0.1 μM) for 6 h, with or without the mTORC1 inhibitor RA (Sigma–Aldrich) or the AMPK inhibitor CC (Sigma–Aldrich). The cells were then stimulated with the immobilized anti-CD3 mAb (3.0 μg/mL) (eBioscience, San Diego, CA, USA) or the immobilized anti-CD3 mAb and soluble anti-CD28 mAb (2.0 μg/mL) (eBioscience) in the presence or absence of TGF-β1 (5.0 ng/mL) (PeproTech, Rocky Hill, NJ, USA). On day 3 after the stimulation with the antibodies, the cells were harvested and cultured with recombinant human (rh) IL-2 (5 IU/mL) (Takeda Pharmaceutical Company, Ltd., Osaka, Japan) for an additional 2 days.

2.6. Flow Cytometric Analysis

Cells were washed and incubated with mAbs for 30 min at 4 °C in 5 mM ethylenediaminetetraacetic acid and PBS containing 2% fetal calf serum [fluorescence-activated cell sorting (FACS) staining buffer]. The following mAbs were used for cell surface marker staining: BV510-conjugated anti-mouse CD3 (Biolegend, San Diego, CA, USA), PE-Cy7-conjugated anti-mouse CD4 (Biolegend), APC-Cy7-conjugated anti-mouse CD4 (Biolegend), APC-Cy7–conjugated anti-mouse CD8α (Biolegend), BV421-conjugated anti-mouse CD25 (Biolegend), APC-conjugated anti-mouse CD103 (Biolegend), PE-Cy7-conjugated anti-mouse KLRG1 (Biolegend), PE-conjugated anti-mouse CTLA-4 (Biolegend), and APC-conjugated anti-mouse GLUT1 (rabbit monoclonal antibody EPR3915, Abcam, Cambridge, MA, USA). A FITC-conjugated anti-mouse IL-10 mAb (Biolegend) was used for intracellular cytokine staining. Intracellular cytokine staining was performed with a fixation/permeabilization kit (BD Biosciences). FITC- or APC-conjugated anti-mouse Foxp3 (eBioscience), FITC-conjugated anti-mouse pS6 (Cell Signaling Technology, CO, USA), and PE-conjugated anti-mouse p-mTOR (BD Bioscience) antibodies were used for intracellular staining using a Foxp3 staining buffer set (eBioscience) according to the manufacturer's instructions. Early apoptosis was detected using annexin-V-FITC and PE (Sigma–Aldrich). Mitochondrial ROS production was detected using MitoSOX-PE (Thermo Fisher Scientific, Kanagawa, Japan). To determine the mitochondrial membrane potential, we used TMRE (tetramethylrhodamine, ethyl ester)-PE (Abcam). TMRE is a cationic, lipophilic dye that accumulates within the mitochondria of healthy cells but not in those that have lost the membrane potential. After staining, the cells were washed, suspended in the FACS staining buffer, and analyzed on a FACS Canto II flow cytometer (BD Biosciences). We determined a suitable gate for lymphocytes (TILs) compared with that of spleen cells. Tumor cells are always larger than TILs, as determined by the forward and side scatter pulse area (FSC-A and SSC-A). The gated populations of lymphocytes (TILs) were identified as $CD4^+CD8^-$, $CD4^-CD8^+$, and double-negative cells. On the other hand, the gate for RLmale1 tumor cells only identified a $CD4^+CD8^+$ population, a unique phenotype of RLmale1 cells as thymus-derived radiation-induced leukemia cells (also express CD3), while other tumor cells never express CD4 or CD8. The numbers of total TILs,

$CD8^+$ TILs, and $CD4^+$ TILs were used to calculate percentages of the populations of these cells among microscopically counted lymphocytes. The numbers of $CD8^+$ TILs and $CD4^+$ TILs were calculated by the % populations of those cells, and the number of lymphocytes was counted microscopically (total TILs).

2.7. Treg Suppression Assay

On day 5 of incubation, iTreg cells were isolated by anti-CD25 magnetic separation (Miltenyi Biotec). $CD4^+$ $CD25^-$ T cells (Tconv) were isolated from wild-type spleen cells and labeled with CFSE (Thermo Fisher Scientific). Irradiated (40 Gray), T cell-depleted splenocytes were used as feeder cells. Tconv and iTreg cells were co-cultured, together with feeder cells containing the anti-CD3 mAb, at different ratios as indicated, and the division of Tconv cells was assessed by dilution of CFSE on day 3.

2.8. Metabolic Assays

OCRs and ECARs were measured in XF medium (non-buffered RPMI 1640 containing 25 mM glucose, 2 mM L-glutamine, and 1 mM sodium pyruvate) in response to 1 μM oligomycin (Sigma–Aldrich, Kanagawa, Japan), 10 μM FCCP (Sigma–Aldrich), and 1 μM rotenone (Sigma–Aldrich) + 1 μM antimycin A (Sigma–Aldrich) using the XFe96 Extracellular Flux Analyzer (Seahorse Bioscience, North Billerica, MA, USA). The proton leakage was calculated according to the following formula: basal respiration − ATP-linked respiration.

2.9. Western Blot Analysis

Cell lysates were prepared by suspending cells in lysis buffer (PBS, 1% Nonidet P-40, 1 mM phenylmethylsulfonyl fluoride). The lysates were cleared by centrifugation and subjected to electrophoresis on a sodium dodecyl sulfate–polyacrylamide gel. The proteins were then transferred to nitrocellulose membranes, blocked with 1–10% dry milk (or bovine serum albumin) in TBS-T buffer [TBS (10 mM Tris–HCl, pH 7.5, 135 mM NaCl) + 0.05% Tween-20]. Antigen–antibody complexes were visualized by chemiluminescence with an enhanced chemiluminescence substrate. Anti-S6 (1:1000), anti-pS6 (1:1000), anti-actin (1:1000) antibodies were purchased from Cell Signaling Technology. Immunoblot images were cut and rearranged to remove irrelevant information; however, all lanes were obtained from the same blots with the same levels of exposure and contrast.

2.10. Sequencing of 16S rRNA Genes

The V3–V4 region of the 16S rRNA gene was amplified as described elsewhere (Klindworth et al., 2013). Mixed samples were prepared by pooling approximately equal amounts of polymerase chain reaction (PCR) amplicons from each sample and subjected to

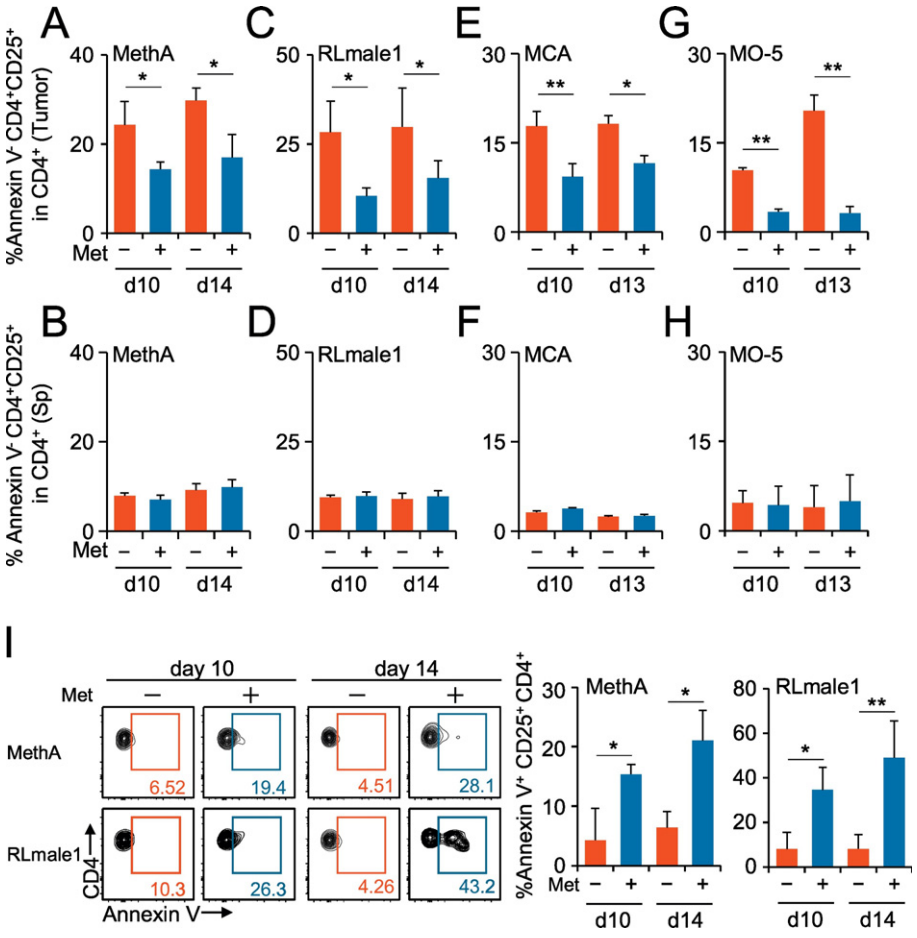

Fig. 1. Metformin (Met)-induced specific reduction of Treg cells in tumors but not in the spleen. Mice inoculated with MethA (A, B), RLmale1 (C, D), MCA (E, F), and MO-5 (G, H) were given Met dissolved in free drinking water from day 7 after the tumor challenge. The tumor and spleen of each mouse were obtained on days 10 and 13 (or day 14), and the TILs and splenic lymphocytes were stained with fluorescence-labeled antibodies to CD3, CD4, and CD25 or with annexin V and subjected to flow cytometry analysis. Annexin V is a reagent that can detect early apoptotic cells. The ratios of the populations of $CD4^+CD25^+$ annexin V^-/$CD4^+$ annexin V^- are shown as bar graphs as indicated. (I) Annexin V positive population of $CD4^+CD25^+$ T cells was shown for Meth A and RLmale1 tumors. Flow cytometry data are produced by pooled TILs from five mice. % annexin $V^+CD4^+CD25^+$ population is shown as bar graphs as indicated. N = 5 for each group. +, Met administered; −, Met not administered; $^*P < 0.05$; $^{**}P < 0.01$. The results are representative of at least three independent experiments.

sequencing by the 2 × 300-base pair protocol with the Miseq platform (Illumina, San Diego, CA, USA) according to the manufacturer's instruction. 16S rRNA reads were analyzed using Quantitative Insights Into Microbial Ecology (QIIME, version 1.8.0). The QIIME pipeline takes raw sequence fastq files and classifies all filter-passed reads of 16S V3–V4 sequences obtained from each sample into operational taxonomic units on the basis of sequence similarity (Sugahara et al., 2015).

2.11. Statistical Evaluation

Student's *t*-test was used for statistical evaluations of normally distributed data.

3. Results

3.1. Tumor Site-Specific Reduction of $CD4^+CD25^+$ Regulatory T Cells by Metformin Administration

To identify tumor-infiltrating $CD4^+CD25^+$ regulatory T cells (Ti-Treg) in tumor homogenates, we used the same gating strategy by which nTreg cells were isolated from the spleen (Suppl. Fig. 1A, B). About 90% of the isolated $CD4^+CD25^+$ Treg population was Foxp3-positive in both spleen and tumor (Suppl. Fig. 1B). A proportional decrease in the Treg/$CD4^+$ T cell ratio was apparent in tumors but not in spleens of the mice taking Met (Suppl. Fig. 2A). Focusing on annexin V^- $CD4^+CD25^+$ T cells (*i.e.*, viable populations), we observed a Met-induced decrease in Ti-Treg populations in four distinct tumors (Fig. 1A to H). This decrease in the number of Tregs in tumors might be explained by the increase in apoptosis of the cells in tumors but not in spleens, as indicated by the expression of annexin V (Fig. 1I, Suppl. Fig. 2B) and cleaved caspase-3 (Suppl. Fig. 3). By contrast, Met administration decreased the expression of cleaved caspase-3 in $Foxp3^-$ conventional $CD4^+$ T cells (Suppl. Fig. 3A). A detailed analysis of one models, the MCA tumor, demonstrated an increase in the annexin V^+ subset of Tregs. Moreover, the absolute number of $CD8^+$ annexin V^- cells per tumor volume (mm^3) increased significantly. Because the number of $CD4^+CD25^+$ annexin V^- cells did not change, Met administration resulted in a significant decrease in the ratio of annexin V^- Ti-Treg to annexin V^- tumor-infiltrating $CD8^+$ T cells (Suppl. Fig. 4). The results suggest that Met administration increases antitumor immunity.

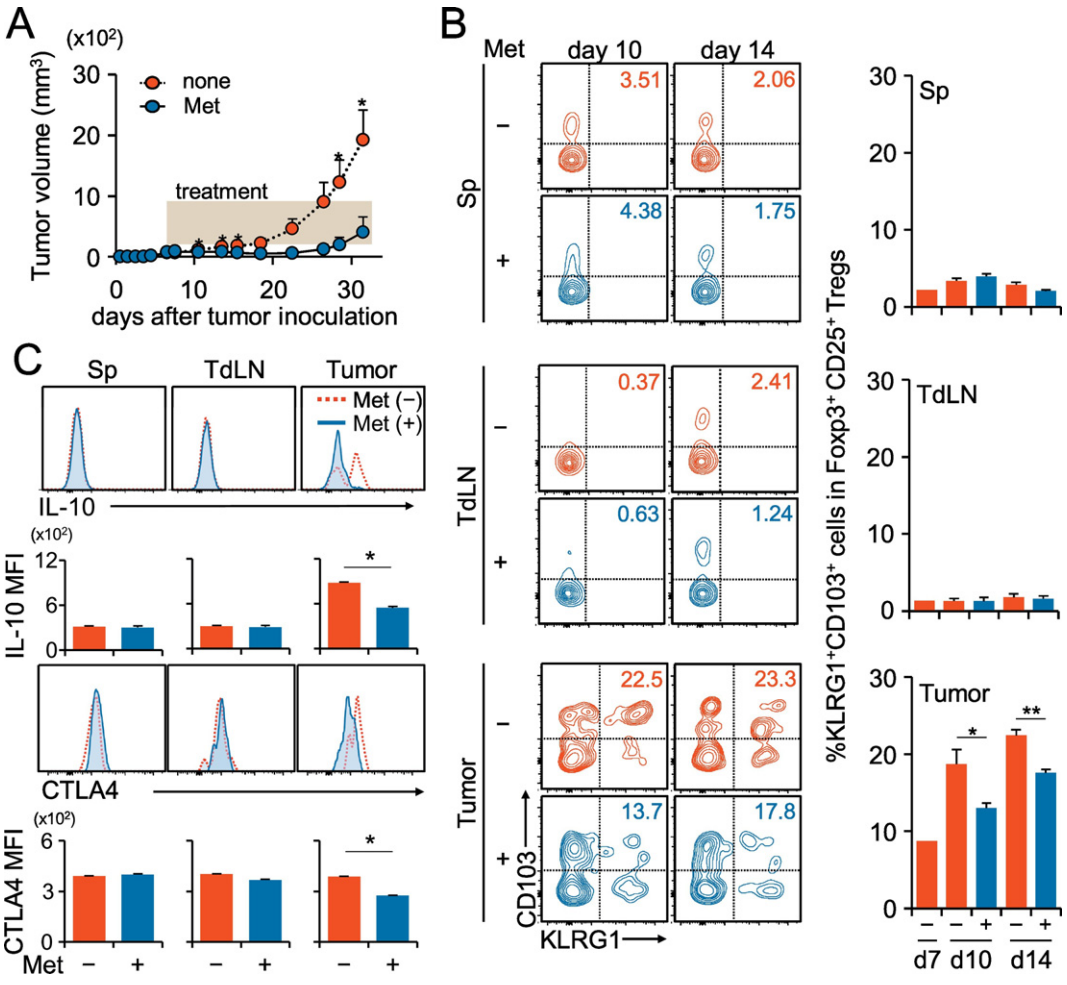

Fig. 2. Decrease of the $KLRG1^+CD103^+$ subpopulation, IL-10 production, and CTLA-4 expression in Ti-Treg cells by Met administration. (A) Tumor growth in mice inoculated with MethA, which were given Met (blue circles) or normal feed (red circles) as indicated by the shadowed rectangle. N = 10 for each group. (B) Terminally differentiated, a $KLRG1^+CD103^+$ population in Ti-Treg cells was reduced by Met administration. Treg subpopulations in the spleen, tumor-draining lymph node (TdLN), and TILs of the MethA-bearing mice were identified by their expressions of KLRG1 and CD103. The experiment was performed twice, and the flow cytometry panels are representative of five independent mice in one experiment. Bar graphs indicate % ratios of the $KLRG1^+CD103^+$ population among $CD4^+CD25^+Foxp3^+$ Treg cells in one experiment. N = 5 for each group. (C) IL-10 production and cell surface CTLA-4 expression were reduced in Ti-Treg cells but not in Treg cells from the spleen, TdLN by Met administration. The cells were pooled from three mice for each group and analyzed by flow cytometry. Mean fluorescence of IL-10 and CTLA4 is shown as bar graphs as indicated. N = 3 for each group. The results are representative of three independent experiments. +, Met administered; −, Met not administered; $^*P < 0.05$; $^{**}P < 0.01$.

3.2. Downregulation of the Effector Molecules of Tumor-Infiltrating $CD4^+$-$CD25^+$ Regulatory T Cells by Metformin Administration

Active effector Treg cells are known to express inhibitory molecules, such as cytotoxic T lymphocyte antigen-4 (CTLA-4) and IL-10 (Laidlaw et al., 2016) and are characterized as a $KLRG1^+CD103^+$ terminally differentiated population (Cheng et al., 2012; Laidlaw et al., 2015). Met administration delayed the tumor growth *in vivo* (Fig. 2A), which was accompanied by the decreased proportion of $KLRG1^+$ $CD103^+$Treg cells in tumors, whereas it did not influence those in tumor-draining lymph nodes (LNs) and the spleen (Fig. 2B). Intracellular cytokine staining of Ti-Treg cells, but not that of the spleen and tumor-draining LNs, revealed a decrease of IL-10 production, and the cell surface level of CTLA-4 was also decreased (Fig. 2C).

Regarding the energy metabolism, Treg generation is fueled by fatty acid oxidation, followed by oxidative phosphorylation in mitochondria (Michalek et al., 2011; Gerriets et al., 2015). Normal mitochondrial function is manifested as appropriate levels of reactive oxygen species (ROS) production and membrane potential. We found a decrease in both the membrane potential and ROS production in Ti-Treg, caused by Met administration (Fig. 3A, B). Interestingly, the cell surface level of a glucose transporter, GLUT1, significantly increased in Ti-Treg cells (Fig. 3C). The results indicated that Met reprogrammed the energy metabolism in Ti-Treg cells, probably shifting to glycolysis rather than oxidative phosphorylation, which might result in a substantially decreased production of IL-10 and a lower expression of CTLA-4.

3.3. Exposure of Naïve $CD4^+CD25^-Foxp3^-$ T Cells to Metformin Results in Decreased iTreg Differentiation, Induced by TCR Stimulation in the Presence of TGF-β

Most tumors are known to produce TGF-β (Derynck and Zhang, 2003), which can be involved in peripheral Treg induction by stimulating *de novo* synthesis of the transcriptional factor Foxp3 and can reduce antitumor immunity (Ghiringhelli et al., 2005; Liu et al., 2007). Therefore, we considered a possibility of disturbed iTreg generation in tumors caused by Met administration. We prepared naïve $CD4^+$ $CD25^-$T cells, which were exposed for 6 h to 10 μM Met, a physiologically relevant plasma concentration in T2D patients who are taking Met (Fig. 4A), and stimulated with anti-CD3 and anti-CD28 monoclonal antibodies (mAbs) with TGF-β for 3 days. Cell division was monitored by labeling the cell surface with carboxyfluorescein succinimidyl ester (CFSE), together with evaluation of the intracellular Foxp3 expression. Met pretreatment accelerated the cell division in both cells treated with the anti-CD3 mAb alone (Fig. 4B, left panel) and anti-CD3 mAb + anti-CD28 mAb (Fig. 4B, right panel). Induction of Foxp3, however, was absolutely dependent on the presence of TGF-β, and surprisingly, it was downregulated by the Met pretreatment as shown in the histograms (Fig. 4B). The ratio of $Foxp3^+/Foxp3^-$ populations did not increase in

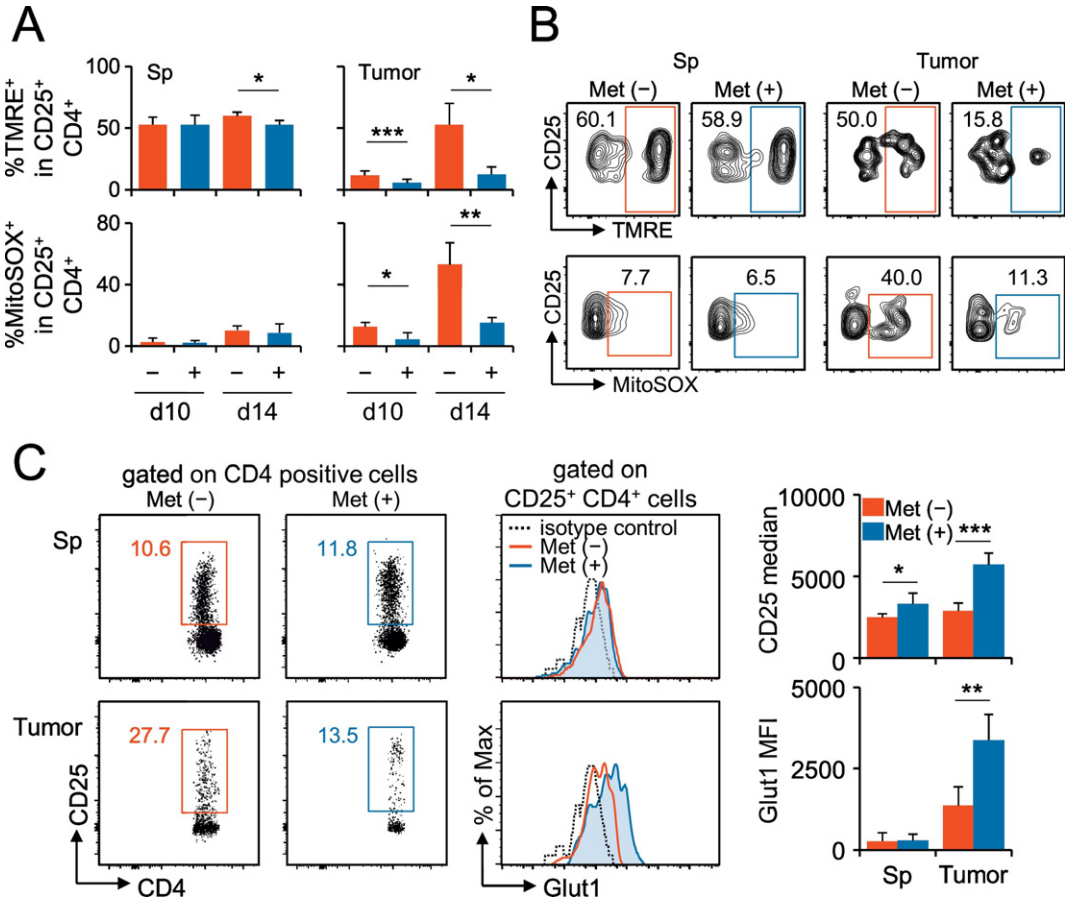

Fig. 3. Met-induced alterations of the mitochondrial membrane potential, ROS production, and GLUT1 expression in Ti-Treg cells. (A) Mitochondrial membrane potential (%$TMRE^+$) and mitochondrial-specific production of ROS (%$MitoSOX^+$) were reduced in Ti-Treg cells of mice bearing MethA by Met administration. The data were obtained from the spleen and TILs of five individual mice in one experiment. The results are representative of two independent experiments. (B) Flow cytometry images on the mitochondrial membrane potential (%$TMRE^+$) and mitochondrial-specific production of ROS (%$MitoSOX^+$) in Treg cells of the spleen and tumor. The results are representative of 10 individual mice from two independent experiments, as in (A), on day10. (C) Cell surface GLUT1 expression was enhanced in Ti-Treg cells by Met administration. Treg cells of the spleen and tumor were examined for their expression of GLUT1. Cell surface GLUT1 expression was monitored in Treg cells from TILs of MethA-bearing mice on day 10 after the tumor challenge. The results were obtained from pooled spleens and TILs of five mice bearing MethA. The bar graph data were obtained from five individual mice. Both results are representative of two independent experiments. +, Met administered; −, Met not administered. $^*P < 0.05$, $^{**}P < 0.01$, $^{***}P < 0.001$.

the Met-treated group by progressive division (Fig. 4C, left and bottom panels). Additional 2 days of culture with IL-2 did not result in any upward trend of the ratio (Fig. 4C, right and bottom panels). In the absence of TGF-β, the ratio of Foxp3$^+$/Foxp3$^-$ populations in both Met-treated and untreated groups was nearly comparable (Fig. 4C, upper graph). The results led us to conclude that the Met exposure suppressed the TGF-β•-induced Foxp3 expression in iTreg cells differentiated from naïve CD4$^+$CD25$^-$T cells. We also examined the CD25 expression in

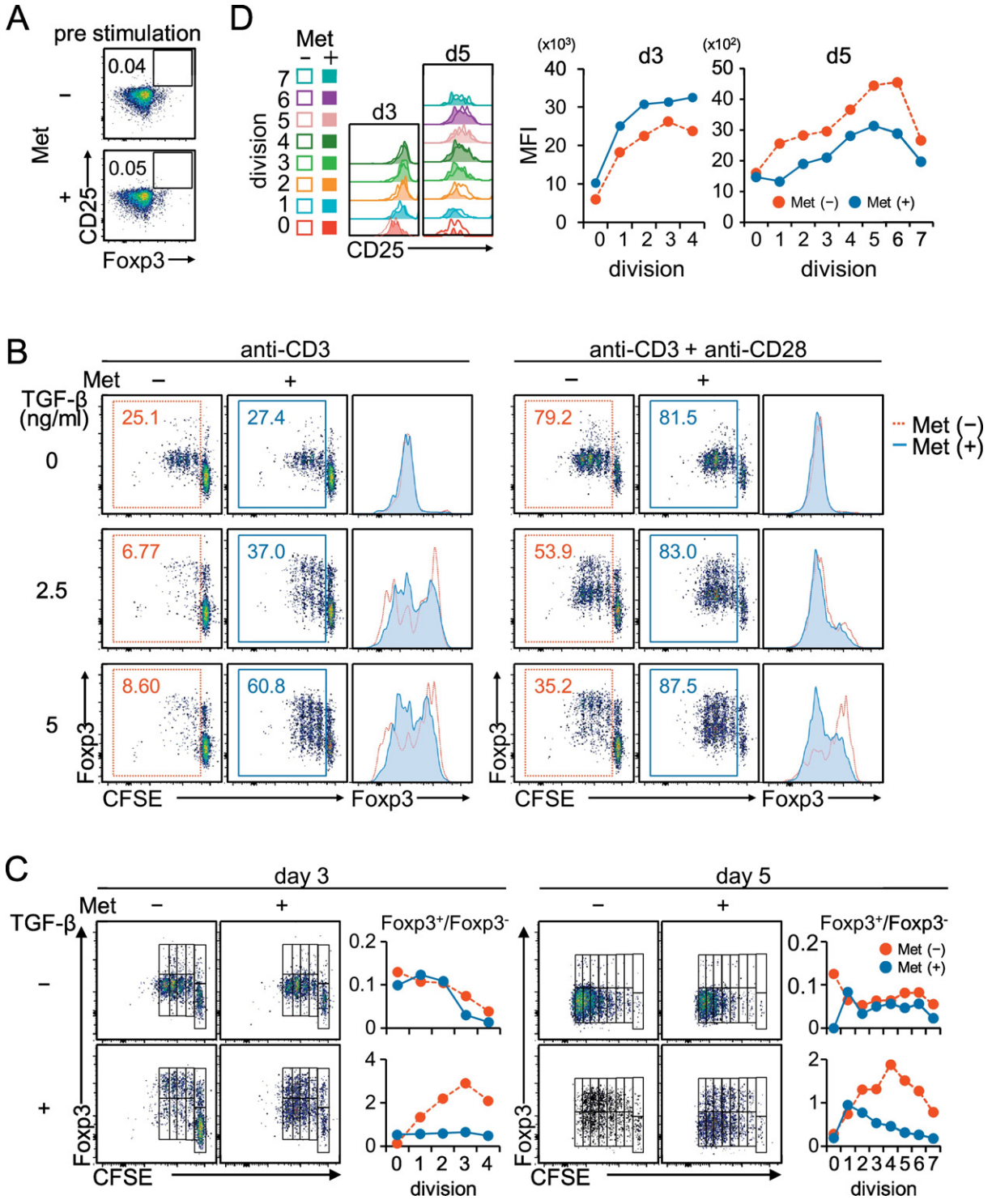

Fig. 4. Met prevents the differentiation of naïve CD4$^+$CD25$^-$ cells into CD4$^+$ CD25$^+$Foxp3$^+$Treg cells. Naive CD4$^+$CD25$^-$ cells purified from BALB/c spleen cells were labeled with CFSE and incubated for 6 h in the presence or absence of 10 μM Met. (A) Met pretreatment of naïve CD4$^+$CD25$^-$ cells did not affect the expression of CD25 or Foxp3. (B) Naive CD4$^+$CD25$^-$ cells pretreated with or without Met as in (A) were stimulated for 3 days with the anti-CD3 mAb or anti-CD3 mAb + anti-CD28 mAb in the presence of graded doses of TGF-β, as indicated. Cell division and Foxp3 expression were monitored simultaneously. Foxp3 expression was significantly inhibited in cells pretreated with Met, as shown in the histograms. (C) The differentiated cells stimulated with anti-CD3 mAb + anti-CD28 mAb in the presence or absence of 5 ng/mL TGF-β as in (B) were expanded for an additional 2 days (day 5) in the presence of IL-2 or analyzed on day 3. The relationship between the number of divisions and the ratio of Foxp3$^+$/Foxp3$^-$ was plotted. No additional increase in the ratio of Foxp3$^+$/Foxp3$^-$ was observed with progressive division of cells pretreated with Met. (D) CD25 expression in Foxp3$^+$ iTreg cells on days 3 and 5 (in C) was examined in parallel with cell division. The results in (A) to (D) are representative of four independent experiments.

Foxp3$^+$ iTreg cells according to cell divisions. The expression level of CD25 increased in parallel with the progressive cell divisions (Fig. 4D). On day 3, the level was further enhanced by pretreatment with Met, while it was downregulated by the additional 2 days of culture compared with the iTreg cells that were not pretreated (Fig. 4D). The implication of this finding is not clear at this stage, although the CD25 level might be associated with the functional activity of Treg cells.

3.4. Functional Reduction and Apoptosis Induction in iTreg Cells Generated From Naïve CD4 T Cells Exposed to Metformin

We evaluated the activity of the iTreg cells on day 5 by a standard suppression assay. As expected, the iTreg cells generated from naïve CD4 T cells pre-exposed to Met showed less suppression against the cell division of conventional CD4 T cells (Fig. 5A). Because of the significant increase of the annexin V$^+$ population among the Ti-Treg cells (Fig. 1I, Suppl. Fig. 2B), we examined the induction of apoptosis in TGF-β-induced iTreg cells. By staining with cell trace violet (CTV) for splenic naïve CD4$^+$ CD25$^-$ T cells purified from Foxp3–green fluorescent protein (GFP) knockin mice (Miyao et al., 2012), we could identify dividing iTreg cells (Fig. 5B, gate a), distinguished from the non-dividing Foxp3–GFP-positive population (Fig. 5B, gate b). The cells in gates a and b were examined for their annexin V binding, and it was revealed that only iTreg cells dividing with IL-2 as an apparent annexin V$^+$ population when they were pre-exposed to Met (Fig. 5B, day 5, gate a).

3.5. Metabolic Reprogramming of iTreg Cells Generated From Naïve CD4 T Cells Exposed to Metformin

The evidence of Met-dependent increase of GLUT1 expression (Fig. 3) inspired us to investigate the metabolic state of iTreg cells. The oxygen consumption rate (OCR, pmol/min) was monitored in CD4$^+$ T cells stimulated with TCR signal as indicated (Fig.6A). We found that Met pretreatment of CD4$^+$ T cells followed by stimulation with anti-CD3 mAb or anti-CD3 mAb and anti-CD28 mAb plus TGF-β increased the basal respiration of T cells and their spare respiratory capacity, as determined by the addition of fluoro-carbonyl cyanide phenylhydrazone (FCCP) (Fig. 6A, upper panel, Fig. 6B, left panel). The upregulation was not observed in the CD4 T cells stimulated with anti-CD3 mAb and anti-CD28 mAb in the absence of TGF-β (Fig. 6A, upper panel, Fig. 6B, left panel), indicating that the metabolic change is linked to TGF-β signaling. Glycolysis, determined by the extracellular acidification rate (ECAR, mpH/min), was also increased in the same manner by the Met pretreatment (Fig. 6A, lower panel, Fig.6B, middle panel). The decreased OCR/ECAR ratio due to the Met pretreatment in iTreg indicates the transition of the metabolic state from oxidative phosphorylation to glycolysis (Fig. 6C). In addition, proton leakage was decreased by the Met pretreatment (Fig. 6B, right panel), probably linked to the decreased ROS production in Ti-Treg cells of the mice receiving Met as shown in Fig. 3A.

3.6. Met-Induced Elevation of mTOR Signaling Impaired iTreg Induction

Next, we tried to find why Foxp3 induction was inhibited in naïve CD4 T cells treated with Met.

Since mTOR signaling is known to act as a negative regulator for Foxp3 induction in naïve CD4 T cells (Zeng and Chi, 2015), it is possible that the Met-induced activation of mTOR took place, resulting in the suppression of the Foxp3 level. To examine this possibility, phosphorylation of a downstream molecule of mTORC1, S6 protein, was examined by western blotting. The elevation of pS6 was apparent in cells pretreated with Met, followed by stimulation with TCR in the presence of TGF-β (Fig. 7A). It was also observed that RA, a specific inhibitor of mTORC1, restored the Foxp3 expression (Fig. 7B). In addition, a similar recovery of Foxp3 by the treatment of cells with CC, an inhibitor of AMPK was found (Fig. 7B). The results indicate that the Met-induced Foxp3 inhibition depends on the activities of both mTORC1 and AMPK, although AMPK activation is known to result in the downregulation of mTOR activity (Gwinn et al., 2008; Tripathi et al., 2013). Neither Met treatment nor inhibitors (RA or CC) affected the original level of Foxp3 in nTreg cells obtained from the spleen (Suppl. Fig. 5); therefore, the effect of Met is restricted to the differentiation of naïve CD4 T cells into iTreg cells. To investigate whether mTORC1 activation occurs *in vivo*, we finally examined the expressions of pS6 on Ti-Treg. We observed a significant elevation of pS6 in Ti-Treg of mice receiving Met compared with that in mice not receiving Met (Fig. 7C). Ti-Treg cells with highest expressions of CD25 was found to contain a larger population of

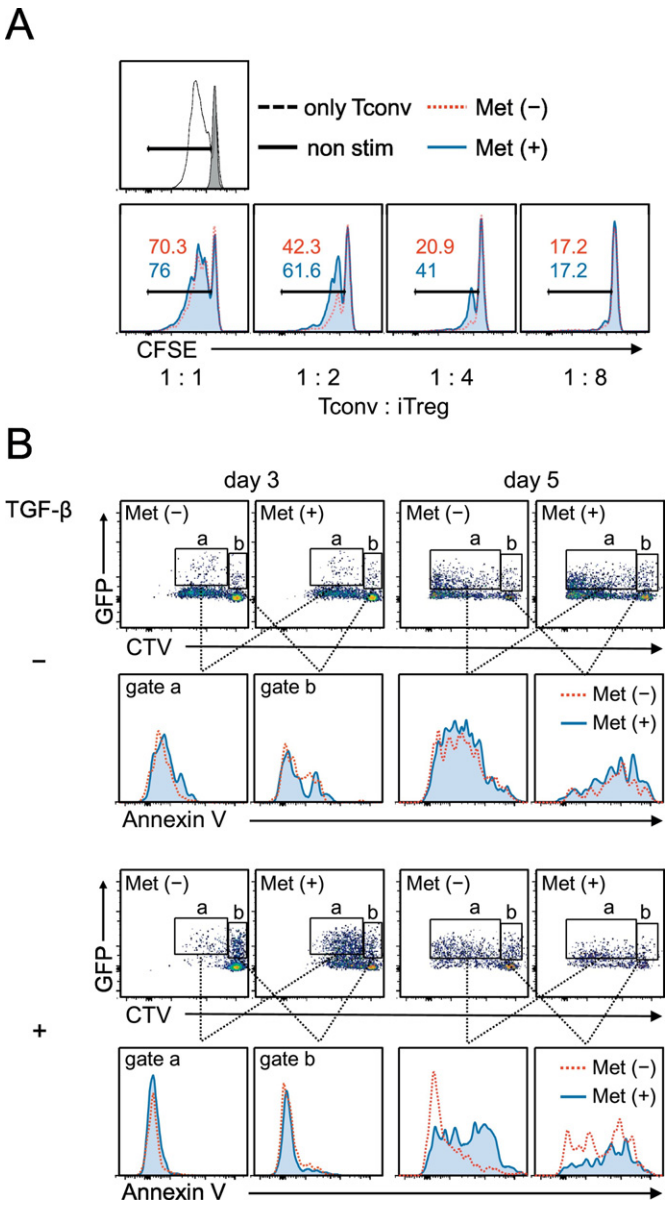

Fig. 5. Reduced inhibitory function and elevated apoptosis of iTreg cells differentiated from Met-treated naïve CD4$^+$CD25$^-$ cells. (A) CD4$^+$CD25$^+$ cells induced as in Fig. 4C (day 5) were enriched in the iTreg cell population using CD25$^+$ magnet beads. iTreg cells were incubated with conventional naïve CD4$^+$CD25$^-$ T cells (Tconv) labeled with CFSE at the indicated ratios in the presence of anti-CD3 mAb and rhIL-2 for 3 days for the Treg suppression assay. iTreg cells that differentiated from naïve CD4 T cells pretreated with Met exhibited less of an inhibitory effect on Tconv cell division. (B) iTreg cells (day 3 and day 5 cultures) were induced from CTV-labeled naïve CD4$^+$CD25$^-$ cells of Foxp3$^{Cre\text{-}GFP}$ mice. The GFP (Foxp3)-positive population was characterized as iTreg cells undergoing cell division (gate a) and those without division (gate b). Only the Met-pretreated iTreg population expanded by IL-2 treatment (day 5, gate a, bottom panel) was positive for annexin V binding, *i.e.*, undergoing apoptosis.

$CD103^+KLRG1^+$ cells, and the p-mTOR levels in the Ti-Treg population was significantly greater in mice taking Met than those in the control mice (Suppl. Fig. 6).

3.7. Met-Induced Metabolic Reprogramming Toward Glycolysis is Linked to Decreased Foxp3 Expression

Because the target of Met is believed to be mitochondrial complex I, we examined the effects of rotenone (Rot) (also known to inhibit complex I activity) on Foxp3 expression. Naïve $CD4^+CD25^-$ T cells were treated with Met or Rot before, after, or before and after TCR stimulation. We found that only treatment before TCR stimulation reduced Foxp3 expression (Fig.7D, Suppl. Fig.7A). The effects of Rot were found to be exactly the same as those of Met (Fig.7D). Since the context-dependent nature of the effect of Met and Rot was puzzling, we examined the metabolic profiles resulting from each treatment condition. We found that an increased ECAR was unique to Met pretreatment and that the OCR/ECAR ratio was significantly lower only with Met pretreatment (Suppl. Fig.7B). These results again suggest that metabolic reprogramming toward glycolysis rather than oxidative phosphorylation is associated with Foxp3 downregulation.

4. Discussion

This report demonstrated a possible contribution of Met in shaping the tumor microenvironment into a favorable state of antitumor

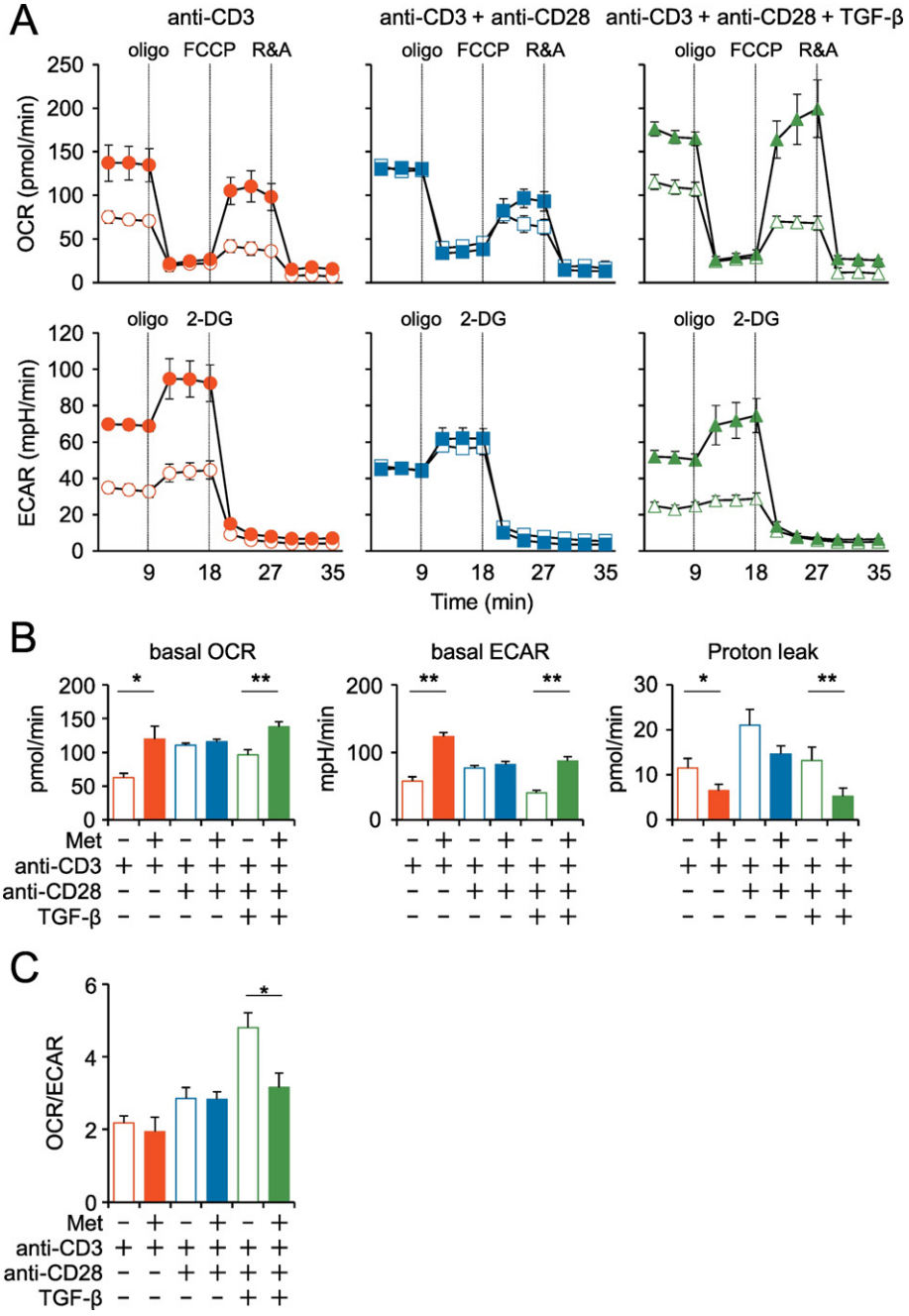

Fig. 6. Metabolic profiles of iTreg cells differentiated from naïve $CD4^+CD25^-$ cells under different conditions. (A) Naïve $CD4^+CD25^-$ cells pretreated with (closed symbols) or without (open symbols) Met were stimulated with antibodies against CD3 or CD3 and CD28 for three days in the presence or absence of TGF-β, as indicated. The OCR and ECAR were assayed using a Seahorse XF96 analyzer with the addition of anti-mitochondrial reagents, oligomycin, FCCP, rotenone (R), antimycin (A), and 2-deoxyglucose (2-DG). Representative data from three independent experiments are shown. (B) Basal levels of OCR, ECAR, and proton leakage are shown under each culture condition as in (A). The ECAR was assayed in Dulbecco's modified Eagle's medium without glutamate. (C) The ratio of ECAR/OCR was plotted as a bar graph. Notably, Met pretreatment decreased OCR/ECAR in iTreg. $^*P < 0.05$; $^{**}P < 0.01$.

immunity through specific reduction of terminally differentiated Treg cells with the KLRG1$^+$CD103$^+$ phenotype. To the best of our knowledge, Met is the only prescribed medicine that can specifically reduce Treg cells at tumor sites, without affecting other peripheral tissues. Regarding mechanistic insight, we demonstrated that Met-pretreatment of naïve CD4T cells inhibits TGF-β-dependent iTreg generation through the activation of mTORC1 followed by the downregulation of Foxp3 expression. In addition to our previous observation suggesting that Met induces reactivation of exhausted CD8 TILs, the present study further reinforces the idea that the immune system mediates the Met-induced anticancer effect. Met treatment is accompanied by a significant reduction of the Treg/CD8 T-cell ratio in a tumor microenvironment, which is associated with a favorable prognosis for cancer patients (Sato et al., 2005).

Only the treatment of naïve CD4T cells with Met or Rot before TCR stimulation resulted in a downregulation of Foxp3 in proliferating CD4T cells. Of note, the presence of Met throughout the experiments did not result in the downregulation of Foxp3. In the Seahorse analysis, we observed that increased glycolysis is a hallmark of Met pretreatment-induced iTreg cells but not of iTreg cells treated with metformin throughout the experiments. The results suggest that the effects observed *in vitro* are caused by a rebound effect and not by any specific effect of pretreatment with Met.

Nonetheless, the context-dependent effects of Met and Rot allowed us to consider what occurs *in vivo* by treating tumor-bearing mice with Met. The intake of Met dissolved in free-access drinking water (5 mg/mL) by mice is known to result in plasma concentrations of approximately 1.7 μg/mL, similar to those of patients with T2D who took Met (0.5–2 μg/mL; Memmott et al., 2010). However, whether the same concentration is reached in the tumor microenvironment is unclear. Recently, Scharping et al. raised the possibility that Met is preferentially incorporated by tumors as opposed to T lymphocytes, as the

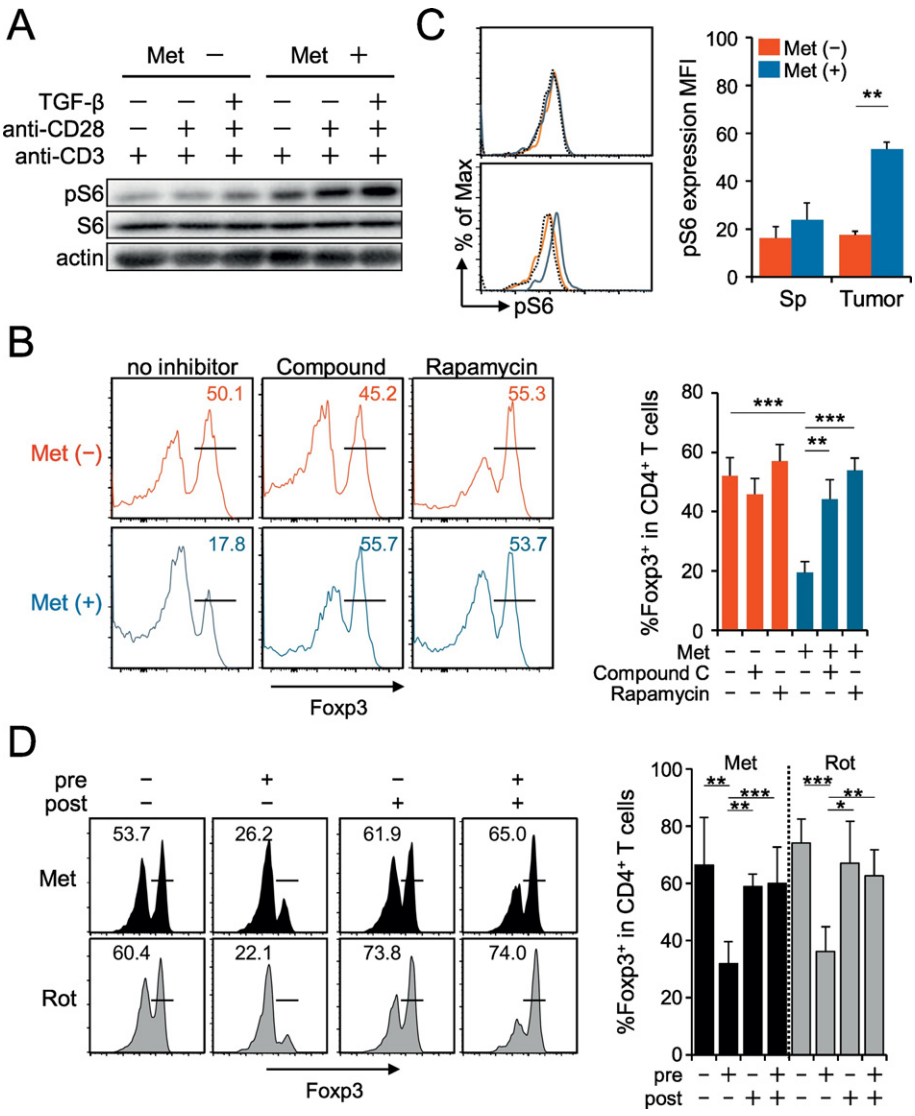

Fig. 7. Involvement of mTORC1 activation in iTreg cells differentiated from Met-treated naïve CD4$^+$CD25$^-$cells. (A) The level of phosphorylated S6 protein (pS6) increased in Met-pretreated naïve CD4$^+$CD25$^-$ T cells in response to different stimulations of TCR for 30 min, as indicated. Each lane includes lysates from 2×10^5 cells. The results are representative of two independent experiments. (B) Foxp3 expression decreased in iTreg cells differentiated from Met-treated naïve CD4$^+$CD25$^-$cells. The presence of rapamycin or compound C during Met pretreatment restored Foxp3 expression. The histogram results are representative of three independent experiments, and the individual results are plotted as a bar graph. N = 3. (C) The level of pS6 protein increased in Ti-Treg cells of mice receiving Met. The histogram data were obtained from pooled spleens and TILs of five mice bearing MethA. The bar graph data were obtained from five individual mice. Both results are representative of three independent experiments. (D) Only Met (or Rot)-pretreatment of naïve CD4T cells before TCR stimulation resulted in a decrease in Foxp3 expression. Pre-treatment assay: CD4$^+$CD25$^-$ T cells were treated with Met (or Rot) for 6 h and washed before TCR stimulation. Post-treatment assay: CD4$^+$CD25$^-$ T cells were treated with culture medium for 6 h and then incubated with Met (or Rot) during TCR stimulation. Three days after TCR stimulation, Foxp3 expression was examined. The histogram results are representative of three independent experiments, and the individual data are plotted as a bar graph. $^*P < 0.05$; $^{**}P < 0.01$; $^{***}P < 0.001$.

expression of the Met transporter OCT-1 (*Slc22a1*) is lower in T cells than in tumor cells (Scharping et al., 2016). This observation indicates that although peripheral blood naïve CD4T cells exposed to Met migrate into tumors, the Met concentration in tumors might be extremely low. Accordingly, naïve CD4T cells exposed to Met in the periphery migrate into tumors and then fail to differentiate into Foxp3-positive regulatory T cells, even with TCR stimulation in the presence of TGF-β. This phenomenon is supported by the finding that *in vitro* iTregs were not generated from naïve CD4T cells that were pretreated with Met. In addition, the authors suggested that oxygenation of the tumor microenvironment by Met may facilitate antitumor immunity elicited by the anti-PD-1 antibody. Oxygen becomes available to the surrounding immune cells since tumor cell respiration is suppressed by Met. Hence, Met-induced increase in oxygen concentration might impact the differentiation/survival and function of T cells, including Treg cells.

Because increased glycolysis is associated with mTORC1 activation, alternative pathways that activate mTORC1 might interfere with the downregulation of Foxp3. In fact, metformin-induced downregulation of Foxp3 is reversed by rapamycin, indicating that mTORC1 activation is essential for the decrease in iTreg generation. Although metformin is known to activate AMPK, resulting in the downregulation of mTORC1 activity; however, this downregulation is not observed *in vivo*. Thus, metformin administration results in the activation of mTORC1, as indicated by enhanced phosphorylation of the downstream S6 protein. Therefore, an alternative pathway that remains to be identified must link the action of metformin to mTORC1 activation *in vivo*. Such a pathway must be associated with the TCR signaling that is mainly activated in tumors but not in peripheral lymphoid tissues. This scenario might occur *in vivo*, which would explain why metformin induces a decrease in Treg in tumors but not in peripheral lymphoid organs. However, this possibility warrants further investigation in future studies.

Seemingly, Met-induced decreased production of IL-10 and a lower expression of CTLA-4 of Ti-Treg cells are associated with metabolic reprogramming toward glycolysis. Evidence of enhanced Glut-1 expression on the cell surface and of decreased mitochondrial membrane potential by Met treatment might support the change of metabolic profile from oxidative phosphorylation to glycolysis. In addition, a recent report suggested that Foxp3 inhibits glycolysis through the suppression of *Myc* gene expression (Angelin et al., 2017), which might support the concept. Further studies are required to elucidate the link between increased glycolysis and decreased IL-10 and CTLA-4 in Ti-Treg cells.

A recent report has indicated that Met treatment of T2D patients affects the gut microbiome (Forslund et al., 2015), and these commensal bacteria regulate the anticancer immune effect induced by a CpG oligonucleotide (Iida et al., 2013) and/or cyclophosphamide (Viaud et al., 2013). In our mouse model, Met is administered by dissolving it in free drinking water. It is possible that oral intake of Met affects the composition of gut microbiota, which regulates the Treg development in the gut (Atarashi et al., 2011; Furusawa et al., 2013), to modulate the immune response against tumors. Therefore, we performed 16S ribosomal RNA (rRNA) sequencing of the fecal microbiota of Met-treated and untreated MO5-bearing mice. Consequently, we found no significant alterations in the fecal microbiota of the mice treated with Met (Suppl. Fig. 8), indicating that the change of intestinal microbiota is negligible.

In summary, we provide compelling evidence that Met, at physiological concentrations, inhibits TGF-β-dependent iTreg generation *in vitro* and attenuates $CD4^+CD25^+$ Treg in tumors, both of which seem to be associated with mTORC1 activation and metabolic reprogramming toward glycolysis. Although the mechanism underlying mTORC1 activation is unclear, these results might help in the development of strategies to control Treg proliferation in a tumor microenvironment.

Funding Sources

This work was supported by grants from Japan Agency for Medical Research and Development (AMED) and the Projects for Development of Innovative Research on Cancer Therapeutics by Ministry of Education, Culture, Sports, Science and Technology Japan (15653356 to H.U. and 26116709 to K.H.) and the Secom Science and Technology Foundation.

Conflicts of Interests

The authors declare no competing financial interests.

Author Contribution

Y.K., S.E. and N.T. designed and performed experiments. Y.F. and K.H. performed 16S rRNA analysis for gut microbiota and analyzed the data. S.D., T.U., S.H., K.H. and A.S. contributed to extensive discussions and critical manuscript reading. H.U. supervised the project and designed the experiments, wrote the paper.

Acknowledgments

We thank Ms. Kondo and Ms. Yamashita for their technical assistance.

Appendix A. Supplementary data

Supplementary data to this article can be found online at https://doi.org/10.1016/j.ebiom.2017.10.009.

References

Adeegbe, D.O., Nishikawa, H., 2013. Natural and induced T regulatory cells in cancer. Front. Immunol. 4, 190.
Angelin, A.L., Gomez, G.D., Dahiya, S., Jiao, J., Guo, L., Levine, M.H., Wang, Z., Quinn III, W.J., Kopinski, P.K., Wang, L., et al., 2017. Foxp3 reprograms T cell metabolism to function in low-glucose, high-lactate environments. Cell Metab. 25, 1282–1293.
Atarashi, K., Tanoue, T., Shima, T., Imaoka, A., Kuwahara, T., Momose, Y., Cheng, G., Yamasaki, S., Saito, T., Ohba, Y., et al., 2011. Induction of colonic regulatory T cells by indigenous *Clostridium* species. Science 331, 337–341.
Boissonnas, A., Scholer-Dahirel, A., Simon-Blancal, V., Pace, L., Valet, F., Kissenpfennig, A., Sparwasser, T., Malissen, B., Fetler, L., Amigorena, S., 2010. $Foxp3^+$ T cells induce perforin-dependent dendritic cell death in tumor-draining lymph nodes. Immunity 32, 266–278.
Cheng, G., Yuan, X., Tsai, M.S., Podack, E.R., Yu, A., Malek, T.R., 2012. IL-2 receptor signaling is essential for the development of $Klrg1^+$ terminally differentiated T regulatory cells. J. Immunol. 189, 1780–1791.
Derynck, R., Zhang, Y.E., 2003. Smad-dependent and Smad-independent pathways in TGF-β family signalling. Nature 425, 577–584.
Eikawa, S., Nishida, M., Mizukami, S., Yamazaki, C., Nakayama, E., Udono, H., 2015. Immune-mediated antitumor effect by type 2 diabetes drug, metformin. Proc. Natl. Acad. Sci. U. S. A. 112, 1809–1814.
Evans, J.M., Donnelly, L.A., Emslie-Smith, A.M., Alessi, D.R., Morris, A.D., 2005. Metformin and reduced risk of cancer in diabetic patients. BMJ 330, 1304–1305.
Facciabene, A., Motz, G.T., Coukos, G., 2012. T-regulatory cells: key players in tumor immune escape and angiogenesis. Cancer Res. 72, 2162–2171.
Fontenot, J.D., Gavin, M.A., Rudensky, A.Y., 2003. Foxp3 programs the development and function of $CD4^+CD25^+$ regulatory T cells. Nat. Immunol. 4, 330–336.
Forslund, K., Hildebrand, F., Nielsen, T., Falony, G., Le Chatelier, E., Sunagawa, S., Prifti, E., Vieira-Silva, S., Gudmundsdottir, V., Krogh Pedersen, H., et al., 2015. Disentangling type 2 diabetes and metformin treatment signatures in the human gut microbiota. Nature 528, 262–266.
Furusawa, Y., Obata, Y., Fukuda, S., Endo, T.A., Nakato, G., Takahashi, D., Nakanishi, D., Uetake, C., Kato, K., Kato, T., et al., 2013. Commensal microbe-derived butyrate induces the differentiation of colonic regulatory T cells. Nature 504, 446–450.
Gerriets, V.A., Kishton, R.J., Nichols, A.G., Macintyre, A.N., Inoue, M., Ilkayeva, O., Winter, P.S., Liu, X., Priyadharshini, B., Slawinska, M.E., et al., 2015. Metabolic programming and PDHK1 control $CD4^+$ T cell subsets and inflammation. J. Clin. Invest. 125, 194–207.
Ghiringhelli, F., Puig, P.E., Roux, S., Parcellier, A., Schmitt, E., Solary, E., Kroemer, G., Martin, F., Chauffert, B., Zitvogel, L., 2005. Tumor cells convert immature myeloid dendritic cells into TGF-β-secreting cells inducing $CD4^+CD25^+$ regulatory T cell proliferation. J. Exp. Med. 202, 919–929.
Gwinn, D.M., Shackelford, D.B., Egan, D.F., Mihaylova, M.M., Mery, A., Vasquez, D.S., Turk, B.E., Shaw, R.J., 2008. AMPK phosphorylation of raptor mediates a metabolic checkpoint. Mol. Cell 30, 214–226.
Halje, M., Nordin, M., Bergman, D., Engstrom, W., 2012. Review: the effect of insulin-like growth factor II in the regulation of tumour cell growth in vitro and tumourigenesis in vivo. In vivo 26, 519–526.
Han, G., Gong, H., Wang, Y., Guo, S., Liu, K., 2015. AMPK/mTOR-mediated inhibition of survivin partly contributes to metformin-induced apoptosis in human gastric cancer cell. Cancer Biol. Ther. 16, 77–87.

Hirsch, H.A., Iliopoulos, D., Tsichlis, P.N., Struhl, K., 2009. Metformin selectively targets cancer stem cells, and acts together with chemotherapy to block tumor growth and prolong remission. Cancer Res. 69, 7507–7511.
Hori, S., Nomura, T., Sakaguchi, S., 2003. Control of regulatory T cell development by the transcription factor Foxp3. Science 299, 1057–1061.
Iida, N., Dzutsev, A., Stewart, C.A., Smith, L., Bouladoux, N., Weingarten, R.A., Molina, D.A., Salcedo, R., Back, T., Cramer, S., et al., 2013. Commensal bacteria control cancer response to therapy by modulating the tumor microenvironment. Science 342, 967–970.
Joshi, N.S., Akama-Garren, E.H., Lu, Y., Lee, D.Y., Chang, G.P., Li, A., DuPage, M., Tammela, T., Kerper, N.R., Farago, A.F., et al., 2015. Regulatory T cells in tumor-associated tertiary lymphoid structures suppress anti-tumor T cell responses. Immunity 43, 579–590.
Klindworth, A., Pruesse, E., Schweer, T., Peplies, J., Quast, C., Horn, M., et al., 2013. Evaluation of general 16S ribosomal RNA gene PCR primers for classical and next-generation sequencing-based diversity studies. Nucleic Acids Res. 41 (1), e1.
Kurose, K., Ohue, Y., Wada, H., Iida, S., Ishida, T., Kojima, T., et al., 2015. Phase Ia study of FoxP3$^+$CD4Treg depletion by infusion of a humanized anti-CCR4 antibody, KW-0761, in cancer patients. Clin. Cancer Res. 21, 4327–4336.
Laidlaw, B.J., Cui, W., Amezquita, R.A., Gray, S.M., Guan, T., Lu, Y., Kobayashi, Y., Flavell, R.A., Kleinstein, S.H., Craft, J., et al., 2015. Production of IL-10 by CD4$^+$ regulatory T cells during the resolution of infection promotes the maturation of memory CD8$^+$ T cells. Nat. Immunol. 16, 871–879.
Laidlaw, B.J., Craft, J.E., Kaech, S.M., 2016. The multifaceted role of CD4$^+$ T cells in CD8$^+$ T cell memory. Nat. Rev. Immunol. 16, 102–111.
Liu, V.C., Wong, L.Y., Jang, T., Shah, A.H., Park, I., Yang, X., Zhang, Q., Lonning, S., Teicher, B.A., Lee, C., 2007. Tumor evasion of the immune system by converting CD4$^+$CD25$^-$ T cells into CD4$^+$CD25$^+$ T regulatory cells: role of tumor-derived TGF-β. J. Immunol. 178, 2883–2892.
Memmott, R.M., Mercado, J.R., Maier, C.R., Kawabata, S., Fox, S.D., Dennis, P.A., 2010. Metformin prevents tobacco carcinogen—induced lung tumorigenesis. Cancer Prev. Res. 3, 1066–1076.
Michalek, R.D., Gerriets, V.A., Jacobs, S.R., Macintyre, A.N., MacIver, N.J., Mason, E.F., Sullivan, S.A., Nichols, A.G., Rathmell, J.C., 2011. Cutting edge: distinct glycolytic and lipid oxidative metabolic programs are essential for effector and regulatory CD4$^+$ T cell subsets. J. Immunol. 186, 3299–3303.
Miyao, T., Floess, S., Setoguchi, R., Luche, H., Fehling, H.J., Waldmann, H., Huehn, J., Hori, S., 2012. Plasticity of Foxp3$^+$ T cells reflects promiscuous Foxp3 expression in conventional T cells but not reprogramming of regulatory T cells. Immunity 36, 262–275.
Morales, D.R., Morris, A.D., 2015. Metformin in cancer treatment and prevention. Annu. Rev. Med. 66, 17–29.
Nair, V., Sreevalsan, S., Basha, R., Abdelrahim, M., Abudayyeh, A., Rodrigues Hoffman, A., Safe, S., 2014. Mechanism of metformin-dependent inhibition of mammalian target of rapamycin (mTOR) and Ras activity in pancreatic cancer: role of specificity protein (Sp) transcription factors. J. Biol. Chem. 289, 27692–27701.
Nishikawa, H., Sakaguchi, S., 2010. Regulatory T cells in tumor immunity. Int. J. Cancer 127, 759–767.
Noto, H., Goto, A., Tsujimoto, T., Noda, M., 2012. Cancer risk in diabetic patients treated with metformin: a systematic review and meta-analysis. PLoS One 7, e33411.
Onizuka, S., Tawara, I., Shimizu, J., Sakaguchi, S., Fujita, T., Nakayama, E., 1999. Tumor rejection by in vivo administration of anti-CD25 (interleukin-2 receptor α) monoclonal antibody. Cancer Res. 59, 3128–3133.
Renehan, A.G., Harvie, M., Howell, A., 2006. Insulin-like growth factor (IGF)-I, IGF binding protein-3, and breast cancer risk: eight years on. Endocr. Relat. Cancer 13, 273–278.
Sato, E., Olson, S.H., Ahn, J., Bundy, B., Nishikawa, H., Qian, F., Jungbluth, A.A., Frosina, D., Gnjatic, S., Ambrosone, C., et al., 2005. Intraepithelial CD8$^+$ tumor-infiltrating lymphocytes and a high CD8$^+$/regulatory T cell ratio are associated with favorable prognosis in ovarian cancer. Proc. Natl. Acad. Sci. U. S. A. 102, 18538–18543.
Scharping, N.E., Menk, A.V., Whetstone, R.D., Zeng, X., Delgoffe, G.M., 2016. Efficacy of PD-1 blockade is potentiated by metformin-induced reduction of tumor hypoxia. Cancer Immunol. Res. 5, 9–16.
Shank, J.J., Yang, K., Ghannam, J., Cabrera, L., Johnston, C.J., Reynolds, R.K., Buckanovich, R.J., 2012. Metformin targets ovarian cancer stem cells in vitro and in vivo. Gynecol. Oncol. 127, 390–397.
Shimizu, J., Yamazaki, S., Sakaguchi, S., 1999. Induction of tumor immunity by removing CD25$^+$CD4$^+$ T cells: a common basis between tumor immunity and autoimmunity. J. Immunol. 163, 5211–5218.
Song, C.W., Lee, H., Dings, R.P., Williams, B., Powers, J., Santos, T.D., Choi, B.H., Park, H.J., 2012. Metformin kills and radiosensitizes cancer cells and preferentially kills cancer stem cells. Sci Rep 2, 362.
Sugahara, H., Odamaki, T., Fukuda, S., Kato, T., Xiao, J.Z., Abe, F., et al., 2015. Probiotic Bifidobacterium longum alters gut luminal metabolism through modification of the gut microbial community. Sci Rep 5, 13548.
Tripathi, D.N., Chowdhury, R., Trudel, L.J., Tee, A.R., Slack, R.S., Walker, C.L., et al., 2013. Reactive nitrogen species regulate autophagy through ATM-AMPK-TSC2-mediated suppression of mTORC1. Proc. Natl. Acad. Sci. U. S. A. 110, E2950–2957.
Viaud, S., Saccheri, F., Mignot, G., Yamazaki, T., Daillere, R., Hannani, D., Enot, D.P., Pfirschke, C., Engblom, C., Pittet, M.J., et al., 2013. The intestinal microbiota modulates the anticancer immune effects of cyclophosphamide. Science 342, 971–976.
Zeng, H., Chi, H., 2015. Metabolic control of regulatory T cell development and function. Trends Immunol. 36, 3–12.
Zheng, L., Yang, W., Wu, F., Wang, C., Yu, L., Tang, L., Qiu, B., Li, Y., Guo, L., Wu, M., et al., 2013. Prognostic significance of AMPK activation and therapeutic effects of metformin in hepatocellular carcinoma. Clin. Cancer Res. 19, 5372–5380.